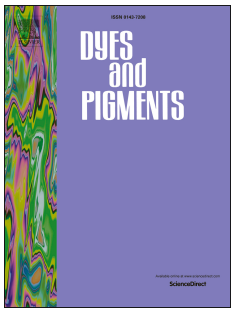

Absorption and fluorescence spectral properties of azo dyes based on 3-amido-6-hydroxy-4-methyl-2-pyridone: Solvent and substituent effects

Slavica J. Porobić, Bojan Đ. Božić, Miroslav D. Dramićanin, Vesna Vitnik, Željko Vitnik, Milena Marinović-Cincović, Dušan Ž. Mijin

PII: S0143-7208(19)31689-4

DOI: https://doi.org/10.1016/j.dyepig.2019.108139

Reference: DYPI 108139

To appear in: *Dyes and Pigments*

Received Date: 18 July 2019

Revised Date: 5 December 2019

Accepted Date: 12 December 2019

Please cite this article as: Porobić SJ, Božić BojanĐ, Dramićanin MD, Vitnik V, Vitnik Ž, Marinović-Cincović M, Mijin DušŽ, Absorption and fluorescence spectral properties of azo dyes based on 3-amido-6-hydroxy-4-methyl-2-pyridone: Solvent and substituent effects, *Dyes and Pigments* (2020), doi: https://doi.org/10.1016/j.dyepig.2019.108139.

All authors conceived of the presented idea. D.Ž. Mijin, M. Marinović-Cincović and M.D. Dramićanin conceived and planned the experiments. S.J. Porobić carried out the experiments. S.J. Porobić, B.Đ. Božić, Ž. Vitnik and V. Vitnik performed the computations. All authors discussed the results and contributed to the final manuscript.

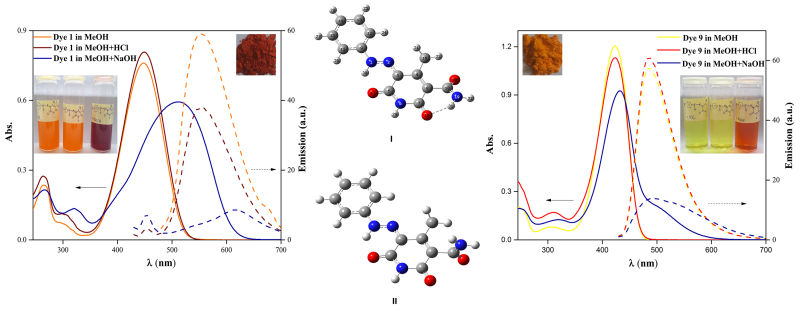

ABSORPTION AND FLUORESCENCE SPECTRAL PROPERTIES OF AZO DYES BASED ON 3-AMIDO-6-HYDROXY-4-METHYL-2-PYRIDONE: SOLVENT AND SUBSTITUENT EFFECTS

Slavica J. Porobić[1], Bojan Đ. Božić[2], Miroslav D. Dramićanin[1], Vesna Vitnik[3], Željko Vitnik[3], Milena Marinović-Cincović[1,*] Dušan Ž. Mijin[4]

[1]*University of Belgrade, Vinča Institute of Nuclear Sciences, P. O. Box 522, 11001 Belgrade, Serbia*

[2]*Institute of Physiology and Biochemistry, Faculty of Biology, University of Belgrade, Studentski trg 16, Belgrade, Serbia*

[3]*Department of Chemistry, Institute of Chemistry, Technology and Metallurgy, University of Belgrade, Belgrade, Serbia*

[4]*Department of Organic Chemistry, Faculty of Technology and Metallurgy, University of Belgrade, Karnegijeva 4, P. O. Box 3503, 11120, Belgrade, Serbia*

Abstract

A series of nine 5-(4-substituted phenylazo)-3-amido-6-hydroxy-4-methyl-2-pyridones were synthesized and characterized by FT–IR, ^{1}H and ^{13}C NMR, UV-Vis, and PL spectroscopy. Photophysical properties of the dyes were examined in solvents of various polarities and at different pH values. The solvent effects on the absorbance and emission spectral shift were analyzed using Lippert–Mataga, Reichardt–Dimroth and Kamlet-Taft equations. Moreover, UV-Vis absorption and emission frequencies were correlated with

* Corresponding Author
E-mail address: milena@vinca.rs

Hammett substituent constants applying the linear free energy relationships. DFT calculations of the investigated dyes were accomplished to determine their structural and electronic properties.

Keywords: Azo pyridone dyes; Absorption spectra; Fluorescence spectra; Solvatochromism; DFT

1. Introduction

Azo colorants represent the most significant class of all colorants [1]. More than 50% of all commercial dyes and pigments belong to azo colorants [2]. This wide usage is due to the simplicity of their preparation as well as to the wide range of colors [3]. They are used in dyeing/textile, leather, pulp, paper, food industry and cosmetics [4]. Azo dyes exhibit antibiotic, antifungal and anti-HIV properties [5]. Also, they found applications in dye-sensitized solar cells [6], biological fluorescence probe development [7], photonics [8], non-linear optical devices [9] and polarizing films [10].

One group of azo colorants, namely those obtained from pyridone moiety (arylazo pyridone dyes), has gained importance in last several decades. Arylazo pyridone dyes are used as disperse dyes, for dyeing synthetic fibers like polyester and nylon [11]. Also, they find application in inks for the heat-transfer printing of polyester [12], in the production of color filters [13] and in printing inks [14].

The photo-physical behavior of a dye dissolved in the corresponding solvent depends on the solvent properties as well as dye-solvent interactions. These interactions influence the intensity, maximum absorption wavelength and shape of the absorption and

fluorescence band [15]. Changes in the position of maximum absorption wavelength, shape and intensity of the absorption spectra can give information on the nonspecific (dielectric enrichment) and specific interactions (e.g. hydrogen bonding) between the dye and solvent molecules.

It is known that fluorescent dyes, which absorb and emit light, have an extremely rigid and extended π-system [16, 17]. Fluorescent dyes find various applications, e.g. for labeling biomolecules, for solid-state dye laser systems, optical fibers, polymer treatment. Substituent nature can influence the fluorescence [18, 19]. Presence of bromine, chlorine, nitro and/or azo group can suppress the fluorescence properties of the molecule [18]. Azobenzenes, in general, can be classified as non-fluorescent while other dye molecules like rhodamines and fluoresceins are highly fluorescent molecules. However, certain derivatives like 2-borylazobenzenes are fluorescent [20, 21]. Although fluorescent azo dyes are rare, there are reports on fluorescence behavior of some dyes with azo group in the molecule [22-24]. Fluorescence behavior was also previously reported for 5-(substituted phenylazo)-3-cyano-6-hydroxy-1-(2-hydroxyethyl)-4-methyl-2-pyridones [25], which led to the alteration of pyridone moiety and improved fluorescence behavior of the dyes presented in this paper.

Arylazo pyridone dyes can exist in two tautomeric forms, azo and hydrazone (Fig. 1). The hydrazone form is usually commercially more valuable since it absorbs light at longer wavelength [26, 27].

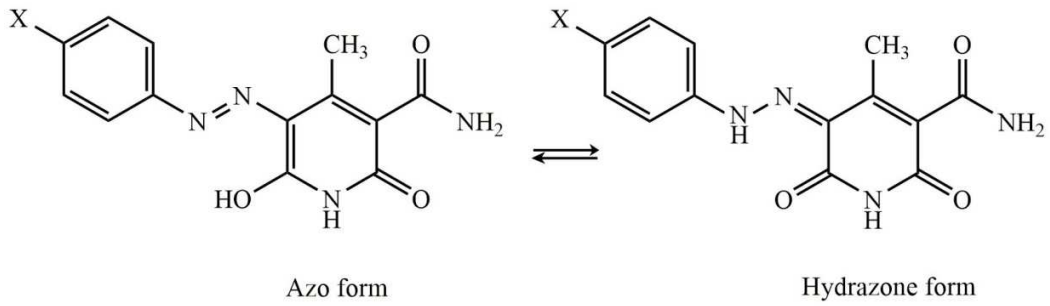

Fig. 1. Azo-hydrazone tautomerism in 5-(4-substituted phenylazo)-3-amido-6-hydroxy-4-methyl-2-pyridones (X=OH (**1**), OCH_3 (**2**), CH_3 (**3**), H (**4**), Cl (**5**), Br (**6**), COOH (**7**), CN (**8**), NO_2 (**9**)).

In this paper, the synthesis of nine 5-(4-substituted phenylazo)-3-amido-6-hydroxy-4-methyl-2-pyridones (five are new) and estimation of their solvatochromic behavior are reported. The absorption and emission spectra were recorded in the range from 300 to 700 nm in fifteen solvents of different features. For the assessment of the solute-solvent interactions and solvatochromic shifts in the UV-Vis and emission spectra of the investigated dyes, Lippert–Mataga, Reichardt–Dimroth equations and the linear solvation energy relationship (LSER) proposed by Kamlet-Taft has been used. For the evaluation of the substituent effects on the absorption and emission spectra, a simple Hammet equation has been employed. Density functional theory (DFT) was used to study the existence and stability of possible tautomers as well as the existence of the intramolecular H-bond between the hydrogen atom of amide group and an adjacent carbonyl group. Also, the structural and spectroscopic characterization (FT-IR and NMR) of dye **4** were done with the help of DFT. Time-dependent DFT method is used for calculation of absorption and fluorescence spectra of all investigated dyes.

2. Experimental

2.1. *Materials and instruments*

All used chemicals were of reagent grade, purchased from Aldrich, Merck, Fisher Chemical, Fluka and Baker, and were used without further purification. The melting points were determined in capillary tubes on an automated melting point system Stuart SMP30. The IR spectra were recorded using a Bomem MB-Series 100 Fourier Transformation-infrared (FT-IR) spectrophotometer in the form of KBr pellets. The ^{1}H and ^{13}C data were obtained using a Varian Gemini 2000 (200 Hz and 50 Hz, respectively) in deuterated dimethyl sulfoxide (DMSO-d_6) and trifluoroacetic acid (CF_3COOD) with tetramethylsilane (TMS) as an internal standard. All spectral measurements were carried out at room temperature (25 ºC). Elemental analysis was performed using a Vario EL III elemental analyzer. The ultraviolet-visible (UV-Vis) absorption spectra were recorded on a Shimadzu 2600 spectrophotometer, while emission spectra were recorded on Fluorescence spectrophotometer Perkin Elmer precisely (LS 45 Luminescence Spectrometer). Relative quantum yields were determined using Rhodamine B in $1 \cdot 10^{-5}$ mol L^{-1} ethanol as standard ($\Phi = 0.7$) [28].

2.2. *Synthesis*

The studied arylazo pyridone dyes (Fig. 1) were prepared from the corresponding diazonium salts and 3-amido-6-hydroxy-4-methyl-2-pyridone toward to before described method [27, 29, 30]. 3-Amido-6-hydroxy-4-methyl-2-pyridone was prepared as published before [29].

The characterization which includes melting point, elemental analysis, FT-IR, ^{1}H and ^{13}C NMR spectra are presented in Supplementary Material.

2.3. *Computational details*

The density functional theory (DFT) calculations of the investigated dyes were performed using Gaussian 09 program package [31] with B3LYP and M06-2X methods with 6-311++G(d,p) basis set. The default convergence criteria were used without any constraint on the geometry. The stability of the optimized geometry was verified by frequency calculations, which gave real values for all the obtained frequencies. Optimized structural parameters were utilized in the calculations of vibrational frequencies, electronic properties and isotropic chemical shifts.

The harmonic frequencies were calculated with B3LYP/6-311++G(d,p) method and then scaled by 0.968 [32]. The assignments of the calculated wavenumbers were helped by the animation option of GaussView 5.0 graphical interface [33] from Gaussian programs, which performed a visual presentation of the shape of vibration modes.

The nuclear magnetic resonance (NMR) chemical shifts calculations were performed using Gauge-Independent Atomic Orbital (GIAO) method, at the same levels of theory in DMSO as solvent. The ^{1}H and ^{13}C isotropic chemical shifts are listed in relation to the corresponding values for TMS. The solvent effect was introduced by the Conductor Polarizable Continuum Model (CPCM). In an attempt to correct the significant deviation between experimental and calculated ^{1}H NMR shift for hydrogen in N–H groups in DMSO-d_6 as solvent, three DMSO molecules were explicitly added in the position that allowed the formation of hydrogen bonds in the molecule.

UV-Vis absorption and fluorescence emission frequencies of dyes were calculated with the TD-DFT method using previously fully optimized geometries in ethanol as solvent. Frontier Molecular Orbitals (FMO) analysis was used to explain the information concerning charge transfer through the dye molecule.

3. Results and discussion

3.1. *Photophysical properties*

To determine the working concentration of the solutions, the electronic spectra of dye **1** in ethanol at five different concentrations were recorded (Fig. 2). The dependence of the absorption maxima of the concentration is consistent with the Lambert-Beer law. Based on the fluorescent spectra at various concentrations of dye **1** in ethanol, as shown in Fig. 2, it is noted that the emission intensity increases to the concentration of $2.5 \cdot 10^{-5}$ mol L^{-1}, after which it starts to decrease. Exactly this concentration ($2.5 \cdot 10^{-5}$ mol L^{-1}) has been chosen as a working concentration for all following experiments. Reduction in emission intensity may be possibly due to concentration quenching which is caused by the formation of aggregates of solute. In general, most organic luminescent materials show luminescence quenching due to self-association of dye molecules in a solvent like ethanol or methanol [34, 35].

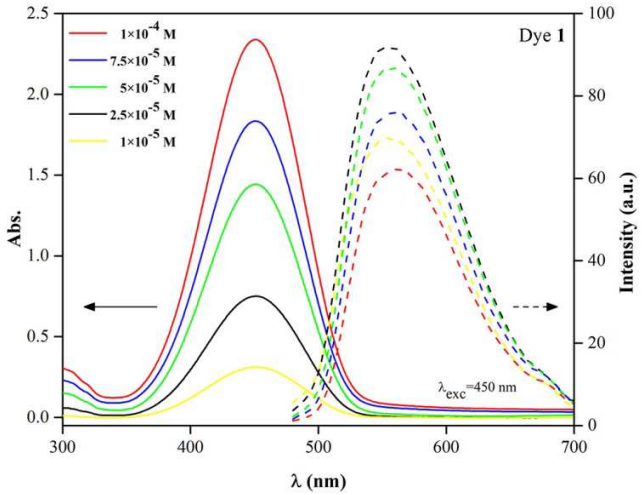

Fig. 2. UV-Vis (full line) and fluorescence (dashed line) spectra of dye **1** in ethanol, at various concentrations in solution.

UV-Vis and fluorescence spectra of the synthesized dyes were recorded in the various solvent to establish the effect of substituents on the absorption and emission properties of newly synthesized dyes. The absorption spectra were recorded in the range of 300-700 nm for all investigated dyes, while fluorescence spectra recording range depends of the absorption maxima. UV-Vis absorption and fluorescence emission maxima of dyes **1**-**9** in a series of solvents of varying polarity and their photophysical properties are shown in Table 1. It has been shown that dyes with electron donor substituent in the *p*-position on the benzene ring (**1**–**3**) shift the absorption and emission maximum to higher wavelengths in all used solvents, while the dyes with electron withdrawing substituents (**4**–**9**) shift the maxima to lower or higher wavelengths depending on solvent properties. Fluorescence quantum yield [28] is also obtained and presented for all investigated dyes (Table S1).

Table 1 Photophysical data of the synthesized dyes in different polarity solvents

	Dye 1				Dye 2				Dye 3			
Solvent	λ_{abs}, nm	log ε, $mol^{-1}dm^3cm^{-1}$	λ_{em}, nm	$\Delta\lambda$, nm	λ_{abs}, nm	log ε, $mol^{-1}dm^3cm^{-1}$	λ_{em}, nm	$\Delta\lambda$, nm	λ_{abs}, nm	log ε, $mol^{-1}dm^3cm^{-1}$	λ_{em}, nm	$\Delta\lambda$, nm
Ethanol	451	4.48	555	104	444	4.44	544	100	429	4.59	515	86
Acetone	444	4.38	549	105	441	4.46	546	105	426	4.78	517	91
DMF	448	4.35	555	107	445	4.46	546	101	425	4.66	517	92
Dioxane	449	4.38	547	98	446	4.51	543	97	431	4.78	516	85
	Dye 4				**Dye 5**				**Dye 6**			
Ethanol	420	4.49	499	79	422	4.50	504	82	420	4.56	506	86
Acetone	417	4.51	499	82	419	4.56	506	87	419	4.53	508	89
DMF	421	4.56	500	79	419	4.85	505	86	420	4.76	508	88
Dioxane	422	4.60	495	73	425	4.81	505	80	425	4.72	506	81
	Dye 7				**Dye 8**				**Dye 9**			
Ethanol	422	4.45	500	78	413	4.37	491	78	423	4.58	485	62
Acetone	416	4.25	490	74	412	4.62	486	74	425	4.67	486	61
DMF	420	4.96	504	84	417	4.81	491	74	432	4.73	488	56
Dioxane	422	4.16	499	77	418	4.87	490	72	427	4.71	489	62

λ_{abs} -absorption maxima, ε – molar extinction coefficient, λ_{em} – emission maxima, $\Delta\lambda$ – Stokes shift

3.2. *UV-Vis and fluorescence spectra of the investigated arylazo pyridone dyes*

The absorption and emission spectra of 5-(4-substituted phenylazo)-3-amido-6-hydroxy-4-methyl-2-pyridone dyes were recorded at room temperature in fifteen solvents of different polarity. The absorption and emission spectra for dyes **1-9** in various solvents are presented in Figs. 3a and 3b, while absorption and emission spectra for representative dyes with electron-donor (Dye **1**) and electron-acceptor (Dye **8**) in different polarity solvents (ethanol and DMF) are given in Figs. 3c and 3d. The characteristic optical spectra for more solvents are presented in Supplementary Materials as Figs. S1-S3. The electronic

spectra confirm that the positions of the UV-Vis absorption and emission wavelengths hinge on the nature of substituent on the phenyl ring of the coupling component and of the solvent properties. Electron-donating substituents (**1**-**3**) in the phenyl ring leads to the bathochromic shift of absorption and emission maxima as compared to the unsubstituted dye (**4**) in all solvents. Electron-withdrawing substituents (**5**-**9**) lead to bathochromic or hypsochromic shifts depending on the solvent polarity. In polar solvents, bathochromic shift has been observed while in non-polar solvents opposite effect has been obtained.

An additional peak that occurs in the emission spectra at about 450 nm for Dyes **1** and **4** in different solvents (*tert*-butanol, 1-butanol, 2-propanol and 1-propanol), probably originates from the anionic form of the molecule (Figs. S1a and S3a). This assumption is made based on observation that the conditions which favorite the formation of the azo anion (Figure 7a) lead to an increase of the peak intensity at 450 nm.

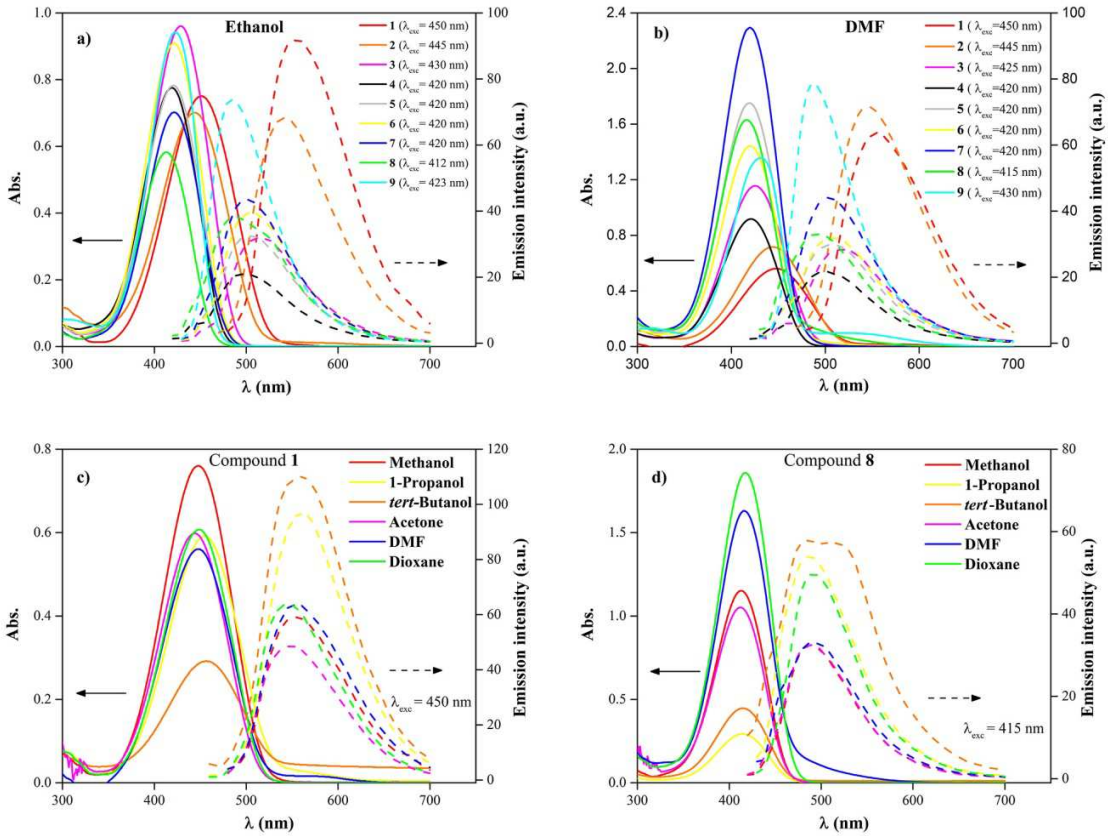

Fig. 3. UV-Vis and fluorescence spectra of dyes **1-9** in ethanol (a) and in DMF (b), dye **1** (c) and dye **8** (d) in various solvents

3.2.1. *Solvent effects on the UV-Vis and emission spectra*

In order to explain the influence of different polarity solvents on fluorescence spectra $\Delta F(\varepsilon, n)$ solvent parameter and Reichardt's solvent parameter E_T were correlated with Stokes shifts.

The change of Stokes shift with solvent polarity can be shown by the Lippert–Mataga plot (Stokes shift - $\Delta F(\varepsilon, n)$ dependence) (Fig. 4), where $\Delta F(\varepsilon, n)$ is calculated from Eq. (1):

$$\Delta F(\varepsilon, n) = [(\varepsilon - 1)/(2\varepsilon + 1)] - [(n^2 - 1)/(2n^2 + 1)] \quad \text{Eq. (1)}$$

ΔF represents the orientation polarizability parameter of the solvent, where ε is the static dielectric constant of the solvent and n is the refractive index of the medium.

The Lippert-Mataga plot was used to investigate the solvent dependent spectral shift [36]. The effect of solvent polarity on the Stokes shift of molecule is a result of the mobility of electrons in the solvent and dipole moment of solvent. The Lippert-Mataga plot for dyes **1**-**9** (Fig. 4) shows satisfactory linear dependence (correlation factor R > 0.97) when only five to nine solvents are included in the correlation. Table S2 (Supplementary Material) contains correlation factor R and solvents included as well as not included in correlation for all investigated dyes. These results highly suggest that the dipole–dipole and dipole-induced dipole non-specific interactions are not solely responsible for the solvent dependent fluorescence shift. The deviation from a linear Lippert–Mataga plot (for more solvents) is an indication that specific interactions (hydrogen bonding) between the dye and the solvent are important interactions in solvation.

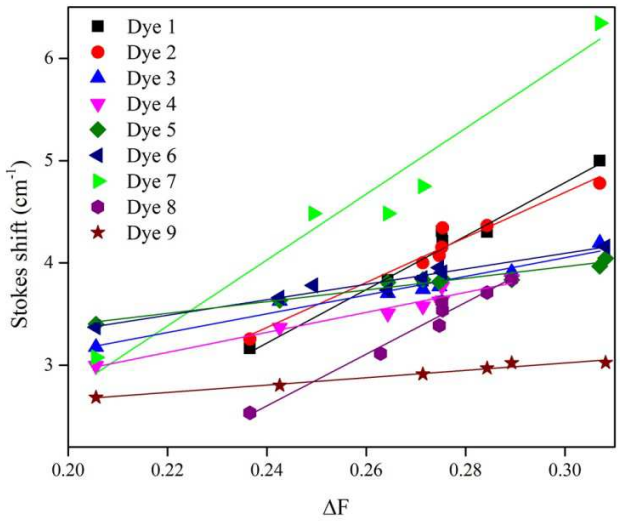

Fig. 4. The Lippert-Mataga plot

Some data from the literature show that the Reichardt-Dimroth scale of polarity is more realistic since it also includes dispersive and specific (hydrogen bonds) interactions [37]. The plot of the Reichardt-Dimroth solvent function *vs.* absorption is shown in Fig. S4. However, this correlation also provides a satisfactory linear dependence only for a small number of solvents. Therefore, solvent effects have to be studied using a multiparameter equation where specific solvent interactions are included in the consideration.

The effect of solvent dipolarity/polarizability and hydrogen bonding on the absorption and emission spectra has been interpreted with a linear solvation energy relationship (LSER) using the Kamlet-Taft solvatochromic equation (2) [38]:

$$\nu = \nu_0 + s\pi^* + b\beta + a\alpha \qquad \text{Eq. (2)}$$

The Kamlet-Taft equation includes parameters which describe dipolarity/polarizability of a solvent (π^*), solvent basicity (β), solvent acidity (α) [39-41] and ν_0 represent the value for solute characteristics in referent solvent (cyclohexane). The regression coefficients s, b and a in Eq. 2 determine the relative susceptibilities of the absorption and emission frequencies to the signified solvent parameters. The solvent parameters used in Eq. (2) are given in Table S3.

The absorption and emission frequencies of the investigated dyes (**1**-**9**) in solvents of different polarity, as well as the values of corresponding Stokes shift, are given in Tables S4-S6, respectively. The correlations of the Stokes shift for hydrazone tautomer have been

performed using multiple regression analysis. The results of the multiple regression analysis are presented in Table 2, and the coefficients v_0, α and β are fitted at the 95% confidence level. The results of the multiple regression using emission and absorption frequencies can be seen in Supplementary (Tables S7-S8). The corresponding percentage contributions of specific and nonspecific effects are given in Table 3 (Stokes shift frequencies), Table S9 (absorption frequencies) and Table S10 (emission frequencies). It is found out, from the analysis of the Stokes shift according to the Kamlet–Taft Eq. (2), that coefficient representing the basicity (β) and dipolarity/polarizability (π^*) of the solvent have a greater influence on spectral properties of the investigated dyes than coefficient representing the acidity (α). The exceptions were observed for dyes **3** and **4** where a slightly greater influence has a parameter α in relation to the parameter π^*. The coefficient representing the hydrogen bond acceptor capability of the solvent has the largest value for dyes **1** and **7**, which indicates that hydrogen atom of the hydroxyl and carboxyl group plays has a major influence in interaction with solvent molecules [42].

For compound **2**, the basicity (β) has been recognized as the most important characteristic of solvent, while remaining parameters α and π have not statistically satisfied conditions.

Table 2 The regression fits to the solvatochromic parameters using the Stokes shift for the investigated dyes

Dye	$v_0 \cdot 10^{-3}$, cm^{-1}	$a \cdot 10^{-3}$, cm^{-1}	$b \cdot 10^{-3}$, cm^{-1}	$s \cdot 10^{-3}$, cm^{-1}	R[a]	S[b]	F[c]	n[d]
1	6.90 (±0.632)	–0.64 (±0.188)	–2.23 (±0.517)	–1.28 (±0.478)	0.9332	0.176	11	9
2*	5.48 (±0.192)	~ 0	-1.82 (±0.252)	~ 0	0.9390	0.111	52	9

3	4.28 (±0.268)	–0.32 (±0.112)	–0.43 (±0.225)	~ 0[#]	0.9010	0.110	10	11
4	4.02 (±0.191)	0.53 (±0.09)	–0.71 (±0.180)	–0.48 (±0.177)	0.9421	0.096	16	10
5	4.59 (±0.209)	0.25 (±0.077)	–0.86 (±0.167)	–0.53 (±0.151)	0.9400	0.071	15	10
6	4.82 (±0.267)	0.20 (±0.106)	–1.17 (±0.229)	–0.41 (±0.217)	0.9053	0.107	10	10
7	3.83 (±0.612)	–0.62 (±0.273)	2.06 (±0.595)	–1.51 (±0.533)	0.9207	0.256	13	11
8	4.43 (±0.308)	0.33 (±0.166)	1.44 (±0.334)	–2.24 (±0.269)	0.9820	0.170	54	10
9	3.41 (±0.140)	0.13 (±0.061)	–0.41 (±0.134)	–0.55 (±0.113)	0.9100	0.072	11	11

R[a]-correlation coefficient, S[b]-standard error of the estimate, F[c]-Fisher's test, n[d]-number of solvents involved in the correlation, * - analysis was performed only with basicity parameter (β), [#] - statistically unreliable data

Table 3 The percentage contribution of the solvatochromic parameters (Eq. 2) using the Stokes shift frequencies.

No.	Substituent	P_{α}, %	P_{β}, %	P_{π^*}, %
1	**OH**	15.51	53.77	30.72
2	**OCH_3**	~ 0	~ 100	~ 0
3	**CH_3**	42.67	57.33	~ 0
4	**H**	30.90	41.11	27.99
5	**Cl**	15.12	52.32	32.56
6	**Br**	11.45	65.49	23.06
7	**COOH**	14.91	49.09	36.00
8	**CN**	8.26	35.95	55.79
9	**NO_2**	11.62	37.45	50.92

Results obtained by the regression analysis using emission frequencies (Table S7) gave negative coefficient *a* (except for the dyes **1** and **9**), *b* (except for dyes **2-5** and **9**) and *s* (except for dyes **4-8**) indicating a bathochromic shift (positive solvatochromism) as well as in absorption spectra due to the increase in polarity, acidity, and basicity of the solvent. This suggests that dipole moment in the excited state is higher than dipole moment in the ground state. The similar behavior was obtained for the results of the regression analysis when the absorption frequencies were used (Table S8).

3.3. *Substituent effects on the UV-Vis absorption and emission spectra*

To quantitate the weights of the substituent effects, the absorbance and emission maxima as well as Stokes shift of 5-(4-substituted arylazo)-3-amido-6-hydroxy-4-methyl-2-pyridone in different polarity solvents were plotted against the Hammett parameter σ_p^+ (Tables 4 and 5; Figs. 5 and 6). The Hammett equation Eq. (3) is an effective way to predict the reaction mechanisms of several organic reactions [2]:

$$v_{max} = v_0 + \rho\sigma_p^+ \qquad \text{Eq. (3)}$$

where ρ is a proportionality constant reflecting the sensitivity of the absorption/emission frequencies to the substituent effect, v_{max} is a substituent-dependent value: absorption and emission frequencies, v_0 is intercept (i.e., describes the unsubstituted member of the series). Given the extended π - conjugation system, electron-donating substituents were expected to stabilize the excited state, thereby explaining the red shifts in the absorbance and emission spectra. [43].

The absorption and emission spectra of the dyes with electron-donating substituents indicate bathochromic shift in all used solvents when compared to dye **4**, while the dyes with electron-withdrawing substituents indicate hypsochromic or bathochromic shift depending on the nature of the used solvent. The ideal relationship between the Hammett constant σ_p^+ and the absorption or emission maxima is linear, regardless of the inductive and resonant increase of the electron density favored by the substituent. Good linear correlations were obtained between the σ_p^+ and emission maxima (Table 5, Figs. 6a and 6b) as well as σ_p^+ and Stokes shift (Table S11). Also, a linear correlation was observed between σ_p^+ and the absorption maxima (Table 4, Fig. 5a), except correlation in aprotic solvents (DMSO and DMF). Non-linear correlation between the Hammett parameter σ_p^+ and absorption maxima in aprotic solvents (Fig. 5b) such as DMSO and DMF indicates a change of the electron density of azo group under the influence of electron-donor and electron-acceptor substituents. In other solvents, the absorption maxima, give linear correlation with the positive values of the constant of proportionality.

A better correlation was obtained with σ_p^+ compared to σ_p (except correlation using Stokes shift), which points to extended delocalization in the arylazo group. The corresponding linear dependency with positive slope confirms the presence of hydrazone form in solvents used for analysis (Tables 4 and 5) [44, 45].

Table 4 The results of the correlation between ν_{max} absorption and σ_p^+ for the investigated arylazo pyridone dyes.

Solvent	ν_{max} vs. σ_p^+	Dye excluded from correlation[a]
Methanol	ν_{max}=23.49+1.125σ_p^+ (R=0.943, n=7)	7, 9
Ethanol	ν_{max}=23.45 +1.346σ_p^+ (R=0.973, n=7)	7, 9

1-Propanol	v_{max}=23.36 +1.346σ_p^+ (R=0.965, n=7)	7, 9
2-Propanol	v_{max}=23.33+1.296σ_p^+ (R=0.934, n=8)	9
1-Butanol	v_{max}=23.32 +1.269σ_p^+ (R=0.925, n=8)	9
tert-Butanol	v_{max}=23.42+1.725σ_p^+ (R=0.948, n=7)	7, 9
1-Pentanol	v_{max}=23.34 +1.408σ_p^+ (R=0.939, n=8)	9
Cyclohexanol	v_{max}=23.36+1.409σ_p^+ (R=0.948, n=8)	9
Benzyl alcohol	v_{max}=23.33 +0.414σ_p^+(R=0.954, n=6)	4, 7, 9
Ethylene glycol	v_{max}=23.38+0.400σ_p^+ (R=0.933, n=5)	3, 4, 7, 9
Acetone	v_{max}=23.67 +1.181σ_p^+ (R=0.968, n=8)	9
Acetonitrile	v_{max}=23.65 +1.038σ_p^+ (R=0.961, n=8)	9
Dioxane	v_{max}=23.79+1.536σ_p^+ (R=0.987, n=8)	9
DMF	D: v_{max}=23.85+1.705σ_p^+ (R=0.991, n=4)	
	A: v_{max}=23.87–0.867σ_p^+ (R=0.963, n=3)	7, 8
DMSO	D: v_{max}=23.82+1.617σ_p^+ (R=0.994, n= 4)	
	A: v_{max}=23.82–1.151σ_p^+ (R=0.977, n=4)	7

[a]Dye number as given in Figure

Table 5 The results of the correlation between ν_{max} emission and σ_p^+ for the investigated arylazo pyridone dyes.

Solvent	v_{max} vs. σ_p^+	Dyes excluded from correlation[a]
Methanol	v_{max}=19.54 +1.434σ_p^+ (R=0.966, n=7)	7, 8
Ethanol	v_{max}=19.53+1.423σ_p^+ (R=0.983, n=8)	4
1-Propanol	v_{max}=19.70+1.623σ_p^+ (R=0.953, n=7)	7, 8
2-Propanol	v_{max}=19.70+1.570σ_p^+ (R=0.954, n=7)	7, 8
1-Butanol	v_{max}=19.68+1.557σ_p^+ (R=0.957, n=7)	7, 8
tert-Butanol	v_{max}=19.84+1.662σ_p^+ (R=0.935, n=7)	7, 8
1-Pentanol	v_{max}=19.70+1.552σ_p^+ (R=0.956, n=7)	7, 8
Cyclohexanol	v_{max}=19.73+1.572σ_p^+ (R=0.952, n=7)	7, 8

Benzyl alcohol	ν_{max}=19.51 +1.498σ_p^+ (R=0.958, n=9)	/
Ethylene glycol	ν_{max}=19.40+1.377σ_p^+ (R=0.964, n=9)	/
Acetone	ν_{max}=19.63 +1.396σ_p^+ (R=0.950, n=9)	/
Acetonitrile	ν_{max}=19.60 +1.401σ_p^+ (R=0.956, n=9)	/
Dioxane	ν_{max}=19.63 +1.273σ_p^+ (R=0.952, n=9)	/
DMF	ν_{max}=19.46+1.387σ_p^+ (R=0.982, n=8)	4
DMSO	ν_{max}=19.79+1.881σ_p^+ (R=0.923, n=8)	9

[a]Dye number as given in Figure 1

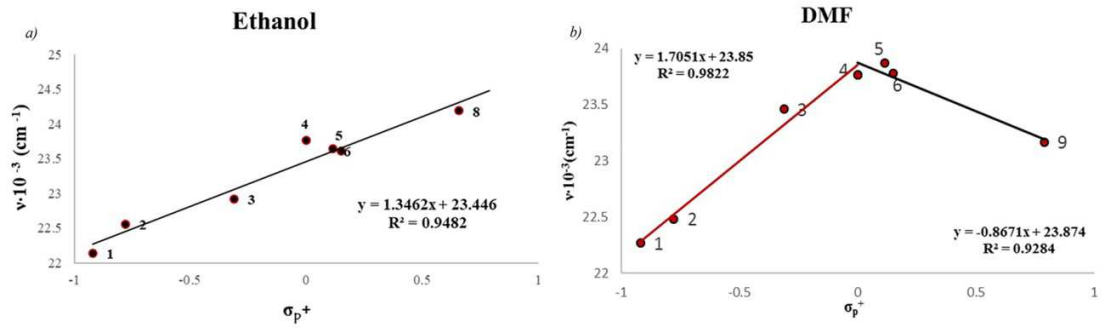

Fig. 5. The correlation between ν_{max} (abs) and σ_p^+ in ethanol (*a*) and DMF (*b*)

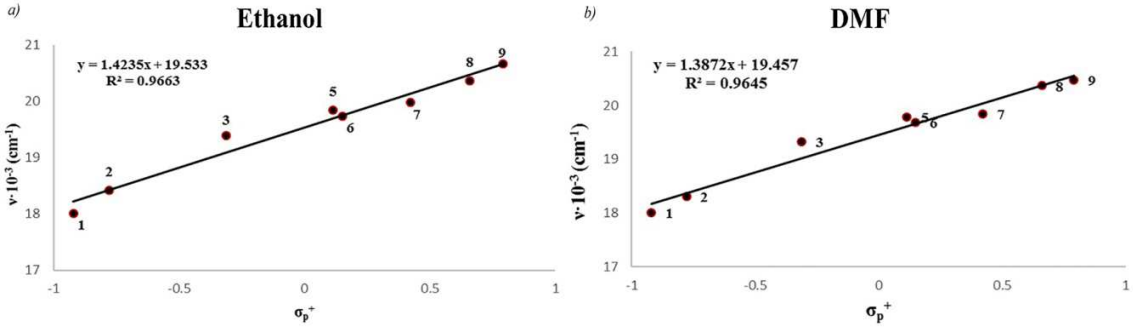

Fig. 6. The correlation between ν_{max} (em) and σ_p^+ in ethanol (*a*) and DMF (*b*)

3.4. *The influence of acidic and alkaline media on azo-hydrazone tautomerism*

The arylazo pyridone dyes presented in this paper may appear in two tautomeric forms (Fig. 1). On the basis of FT-IR and NMR spectra, it was concluded that prepared dyes are in hydrazone form. It is known that the azo-hydrazone tautomerism as well as azo anion- hydrazone equilibrium is influenced by changing the solvent, or by changing the pH of the reaction mixture [46, 47]. In addition, the influence of pH on the azo-hydrazone tautomerism and azo anion-hydrazone equilibrium of the investigated dyes was examined. The pH of the dye solution was adjusted using the solutions of acid or base. The recorded UV-Vis and fluorescence spectra of dyes **1** and **9** in methanol as well as in acidic and alkaline medium are presented in Fig. 7.

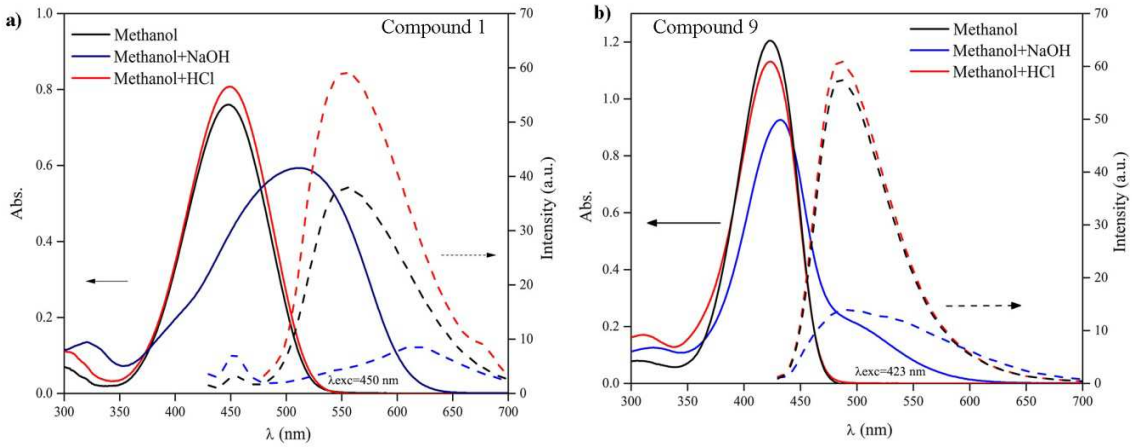

Fig. 7. UV-Vis and fluorescence spectra of dyes **1** (a) and **9** (b) in methanol, as well as in the acidic and alkaline medium

As can be seen from the spectra given in Fig. 7, the selected dyes show similar spectral features in the UV-Vis region in methanol and in acidic media which confirms that dyes appear in hydrazone form. When the solution of dye **1** was made alkaline by the

addition of sodium hydroxide, a significant bathochromic shift was recorded in absorption spectra due to the formation of azo anion form [47]. In the absorption spectra of dye **9** in alkaline methanol, there is equilibrium between hydrazone form and azo anion form, with dominant hydrazone form. For dye **1**, it seems that azo anion form is dominant. On the other side, the intensities of the fluorescence spectra in alkaline media are much lower than in pure methanol and acidic methanol.

3.5. DFT study

3.5.1. Conformational analysis

Because of the presence of two acidic hydrogen atoms, which can migrate between seven positions suitable for their binding, the investigated molecules can exist in several tautomeric forms. From our previous studies on similar systems [47-49] the most stable tautomeric forms belong to azo and hydrazone types, which are shown in Fig. 1. Also, the investigated molecules possess amide group which can participate in both intra- or intermolecular hydrogen bonding (with adjacent carbonyl group and/or solvent molecules) and form, at least, two different conformations, with or without intramolecular H-bond. Therefore, in this research, several goals were set: determining the most stable tautomer, determining the geometry of its stable conformers, as well as their relationship with the electronic properties of the ground and excited state of the investigated molecules.

The appropriated tautomers are defined on the basis of our recent results for similar molecules [48] in which the nine tautomers are identified and approved. Also, the newly introduced amide group also provides a suitable place for the migration of acidic hydrogen. The additional four tautomers may be generated when the hydrogen atom is migrated to its oxygen or nitrogen atom. These tautomers are especially studied in order to determine their stability in comparison to the most stable tautomer and to check its possible presence in the mixture.

It can be seen from the CPCM(ethanol)/M06-2X/6-311++G(d,p) calculation of all defined tautomeric forms for dye **4** that the first set of the nine tautomers are identified and approved as stable and the energy relations are similar as in previous investigation [48]. The most stable geometries belong to the hydrazo tautomeric form (see Fig. 8) while the second most stable form belong to azo tautomer. The energy difference between these two forms is 7.2 kcal/mol. The obtained results are consistent with the previous reports [48, 50, 51]. Also, the calculations showed that migration of acidic hydrogen to nitrogen atom of amide group can't produce stable tautomeric form while the migration to oxygen atom produces stable tautomers with energies higher than 11 kcal/mol, in comparison to hydrazone tautomer. Therefore, only the geometries of the hydrazone form are used for further geometry and electronic study of all investigated dyes.

Most of the tautomers with respect to the mutual orientation of the amide group can exist in two conformational forms. The first, with amide group in almost parallel position to molecule forms the intramolecular H-bond with adjacent carbonyl group while the second with group orientation normal to the plain of molecule is without intramolecular H-bond. Calculations confirm that most stable tautomer can exist in both conformational forms and

energy difference between them is just ~0.19 kcal/mol. Therefore, it can be concluded that both conformers are present in an almost equimolar ratio in the solution, at room temperature. The geometries for both conformers of most stable hydrazone tautomer of dye **4**, fully optimized at M06-2X/6-311++G(d,p) are presented in Fig. 8. The energies (E), relative energies (ΔE) and statistical Boltzmann distribution weights (ω) for all isomers of dye **4** are given in Table S12 supporting information.

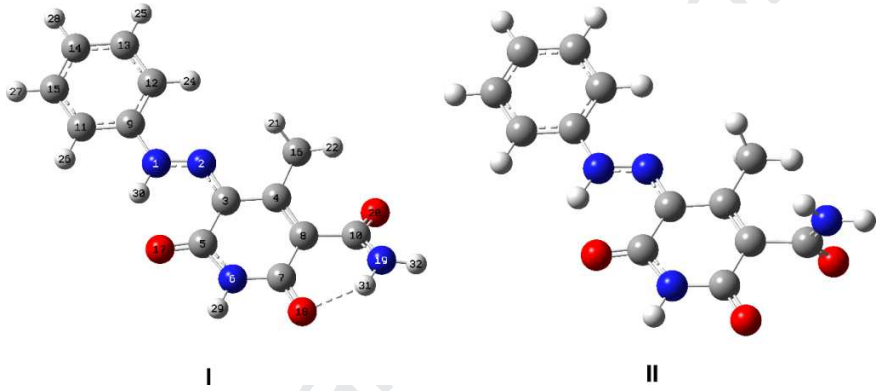

Fig. 8. The geometries of conformer **I** and **II** of the most stable hydrazone tautomeric form of dye **4**.

Since these results are not in correlation with ^{1}H NMR results which indicate the presence of just one conformer, we decided to explore reasons for this discrepancy and if possible, offer a solution for such cases.

The H-bond is supposed to be weak, because the NH_2 group is a weak H-bond donor and according to the classification of Jeffrey [52] that the stabilization energy for weak hydrogen bonds is 1–4 kcal/mol, the intramolecular H-bond in the investigated dyes may be classified as weak or very weak H-bonds. Our previous studies on similar systems [53] revealed that different media (solvents) may strongly influence the nature and the structure of hydrogen bonds. In the same time, there are many proofs that the standard

continuum solvent models cannot adequately treat effects that proton donating and/or accepting solvents may have on the geometry of solute. The continuum dielectric solvent model only implicitly mimicked the solute-solvent H-bond(s) by the polarization of the solvent and concomitant appearance of surface charges on the inner surface of the cavity. This response is qualitatively correct, but the calculated solute-solvent stabilization energy is underestimated. For real determination of the free energy changes in the case of dissolving a polar solute in a protic solvent, intermolecular H-bonds are required [54].

To explore these findings, the potential energy scan (PES) for rotation of the amide group was done by B3LYP and M06-2X methods and 6-311++G(d,p) basis set. The impact of implicit solvent is simulated with CPCM model for simulation of ethanol and DMSO as solvents, and one explicit molecule of ethanol or DMSO is added in the vicinity of amide N-H for simulation of intermolecular H-bond. The mixed implicit model with one explicit solvent molecule model is tested too. During the calculation, all the geometrical parameters were simultaneously relaxed while the C7-C8-C10-N19 torsion angle was varied from 0 to 360° in steps of 5°. The truncate PES's from B3LYP/6-311++G(d,p) calculations in vacuum and ethanol are shown in Fig. 9. The full PES's for B3LYP and M06-2X calculation in vacuum, ethanol and DMSO are presented in Figs. S5-S7.

From Fig. 9 it can be seen that the B3LYP calculation in a vacuum is not capable of locating a conformer without an intramolecular H-bond (**II**). The explicit addition of one molecule of solvent only slightly improves the behavior of the PES from the calculation in a vacuum. It is a logical assumption that a full solvation sphere around a dissolved molecule should be defined for proper treatment of the conformers when the calculation in

vacuum is used, and that is a very demanding task for QC methods. So, using this model, it is possible to properly treat only molecules in the gas phase and non-polar solvents.

The PES, obtained from the B3LYP calculation in which CPCM model (implicit solvent) is used for simulation of ethanol as a solvent, exhibits significantly better behavior and show that such method is capable of locating geometry with intramolecular as well as H-bond free geometry, although the stabilization energy due to the solvation of such conformer is significantly underestimated.

The introduction of an explicit solvent in the form of one ethanol molecule changes the energy relationship between the conformers, i.e. reduces the energy of the conformer **II** in relation to the conformer **I** by 0.51 kcal/mol, i.e. 0.55 kcal/mol in DMSO (energy is given as the difference between the ZPE corrected energies for fully optimized conformers).

The number of explicit solvent molecules taken into consideration as first solvation shell is of crucial importance [55-57]. We believe that the proper first solvation shell around the amide and carbonyl groups involved in the formation of an intramolecular bond should include four ethanol molecules (or two DMSO molecules) to represent all strong solute-solvent interactions of conformer **II** [57]. This would certainly lead to additional stabilization of conformer **II**. At the same time, the introduction of additional explicit molecules would lead to problems with the clustering of solvent molecules, and thus to incorrect treatment of the energy relations of the systems with an inconsistent number of solute-solvent H-bonds. However, based on the assumed tendency of increasing stabilization with establishing additional intermolecular H-bonds, it can be said that conformer **II** represents the dominant conformational form of molecule **4** in solvents that

can participate in H-bond formation as either donors and/or acceptors, such as ethanol and DMSO.

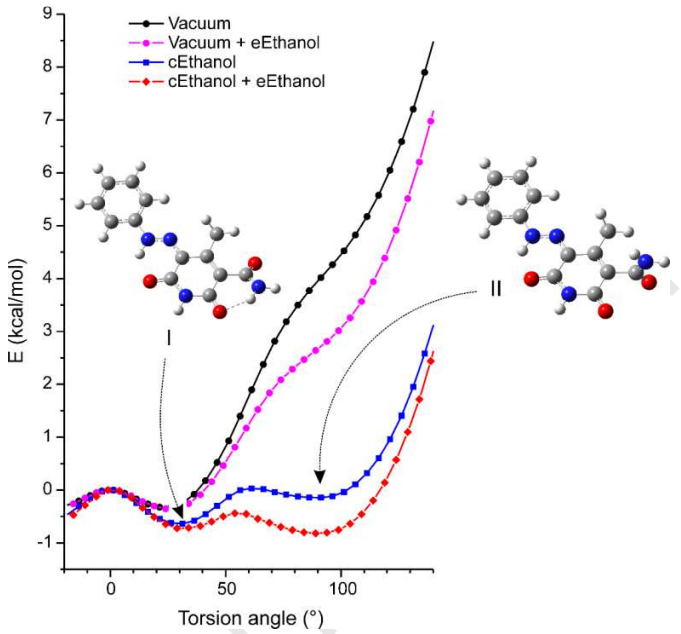

Fig. 9. The PES's for rotation of amide group from B3LYP/6-311++G(d,p) calculations in vacuum and ethanol.

3.5.2. *Vibrational analysis*

Detailed analysis of experimental and calculated infrared spectra of unsubstituted dye **4** has been done in an attempt to shed light on its structure. The most significant wavenumbers are tabulated in Table S13, and the comparison of the experimental and calculated spectra is presented in Fig. 10. Numeration of dye **4** is given in Fig. 8.

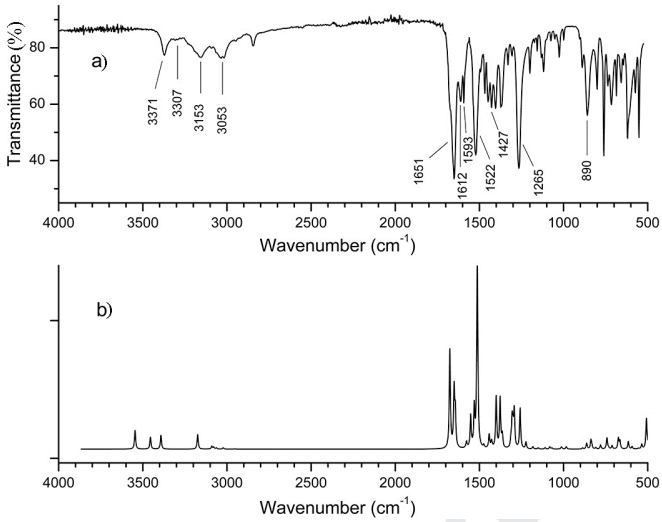

Fig. 10. Comparison of experimental (a) and scaled theoretical (b) IR spectra of the investigated dye **4**

As the structural analysis confirmed, the most stable tautomeric form of the investigated dyes is hydrazone form. So, in the following analysis, vibration frequencies of hydrazone tautomer of dye **4** calculated at B3LYP/6-311++G(d,p) level are compared with experimental ones.

In experimental spectrum, two broad bands at 3153 and 3371 cm^{-1} are assigned to symmetric and asymmetric stretching vibrations of amide $N19H_2$ group. These assignments are supported by scaled theoretical values 3397 and 3551 cm^{-1} (mode nos. 88 and 90), respectively. The most important bands in the region 2800-3600 cm^{-1} are stretching bands of N1−H30 and N6−H29 group at 3053 and 3307 cm^{-1} belong to hydrazone and pyridone moieties and correlate well with the calculated values 3178 and 3459 cm^{-1} (B3LYP mode nos. 87 and 89) as well as with literature data [49]. The bands at 3026 and 3034 cm^{-1} in FT-IR are assigned to aromatic C−H asymmetric and symmetric stretching vibrations. In this region two bands at 2845 and 2947 cm^{-1} origin of symmetric and asymmetric stretching

vibrations of methyl $C15H_3$ group and correlate well with calculated values 2958 and 3026 cm^{-1}, respectively.

The most significant stretching bands are at 1593, 1612 and 1651 cm^{-1} assigned to stretching vibrations of carbonyl C5=O17, C7=O18 and C10=O20 group, respectively and correlate with calculated values at 1645, 1652 and 1678 cm^{-1} (mode nos. 76, 77 and 78). The appearance of these bands in FT-IR spectrum confirms the existence of hydrazone tautomeric form of dye **4**. The bands observed at 552 cm^{-1} and 890 cm^{-1} in FT-IR spectrum are assigned to in-plane bending modes of three carbonyl groups, and the corresponding scaled calculated values are 508 and 863 cm^{-1}.

Two others characteristic hydrazone group vibrations are stretching C3=N2 and bending N1−H30 group vibrations. They are expected in the region 1300–1500 cm^{-1}. The bands observed at 1331-1522 cm^{-1} have contributions from the C3=N2 stretching and N1−H30 in plane bending modes and agree well with the calculated data at 1294-1514 cm^{-1}. The calculated wavenumbers 1013 and 1083 cm^{-1} depicted in Table S13 are assigned as rocking vibrations of $C15H_3$ and $N19H_2$ group, respectively and their experimental counterparts are observed at 1026 and 1157 cm^{-1}.

The bands observed at 687 and 858 cm^{-1} are identified as out-of-plane bending vibrations of N6−H29 and N1−H30 group, respectively, and show good agreement with calculated data, Table S13. This analysis supports the existence of dye **4** in the hydrazone tautomeric form.

3.5.3. *NMR spectral analysis*

Additional proof of the hydrazone tautomeric structure was provided by the NMR spectral analysis. Full geometry optimization of dye **4** was performed with B3LYP/6-311++G(d,p) method and then (GIAO) chemical shift calculations have been made by the same method. The ^{1}H and ^{13}C chemical shifts are measured in DMSO-d_6 and presented in Table S14 and S15. The recorded ^{1}H and ^{13}C NMR spectra of **4** are shown in Figs. S8 and S9.

In the ^{1}H NMR spectrum the chemical shift values for hydrogen H21, H22 and H23 of methyl group are 2.41, 2.13 and 2.44 ppm (with respect to TMS) and correlate well with experimental singlet peak at 2.23 ppm. The aromatic C–H signals are observed at 7.2-7.53 ppm and calculated values are in region 7.45-8.97 ppm. The ^{1}H chemical shifts of two protons of NH_2 group are observed at 7.57 and 7.71 ppm and correlate well with calculated values at 8.97 and 8.98 ppm. The NH hydrogen of pyridone moiety appears at 11.68 ppm, and is determined computationally at 12.57 ppm. The singlet observed at 14.25 ppm is assigned to hydrogen H30 of hydrazone group, which has been calculated at 14.42 ppm.

A solvent like DMSO-d_6 may be treated as a hydrogen bonding partner, which results in changes in the chemical shifts of a certain group of protons, like NH_2 group [55]. In our present work, the spectra recorded in this solvent do not show many changes in ^{1}H NMR. The shift is more substantial for NH_2 group. This is due to the strong hydrogen bonding of the polar amide $CONH_2$ group to the sulfoxide oxygen, which simultaneously deshields the amino protons and impedes rapid proton exchange that would prevent the occurrence of spin-spin splitting.

In the aliphatic region of ^{13}C NMR spectrum, one signal at 14.52 can be ascribed to the carbon atom of methyl group $C16H_3$. The peaks observed in region 116.32-129.92 ppm are assigned to aromatic carbon atoms and correlate with calculated shifts in region 120.36-137.72 ppm. Two carbon atoms C4 and C8 of pyridone ring resonating at 145.59 and 125.49 ppm in the ^{13}C NMR spectra show good agreement with computed values 134.62 and 158.17 ppm, in DMSO solution. Carbon atom C3 of hydrazone group appears at 125.08 ppm, and the calculated value is 131.29 ppm. Two peaks at 162.00 and 162.25 ppm are ascribed to carbonyl carbon atoms C5 and C7 with calculated values at 170.03 and 172.26 ppm. The peak at 166.63 ppm is assigned to another carbonyl group, which is a part of amide group of dye **4**. The counterpart of this signal in the calculated spectrum is at 177.98 ppm.

3.5.4. Calculated UV-Vis and fluorescence spectra of the investigated arylazo pyridone dyes

Calculated absorption and photoluminescence spectra were analyzed to gain insight into the electronic structure of investigated molecules. Tables 6 and 7 describe the relative energies, intensities and absorption wavelengths of investigated dyes calculated at B3LYP and M06-2X/6-311++G(d,p) level, respectively. The band positions of the calculated fluorescence spectra at B3LYP/6-311++G(d,p) level are listed in Table 8 along with experimental band positions for comparison. Conformation analysis showed that the conformer without intramolecular H-bond (**II**) in ethanol as a solvent is more stable than that with intramolecular H-bond (**I**). Despite that and for the purpose of comparison, the UV-Vis and fluorescence spectra for both conformers of dyes **1**-**9** are calculated.

Figures S10 and S11, in Supporting Information file, plot the experimental against the calculated UV-Vis absorption of conformers **I** and **II** of dyes **1**-**9**, calculated at B3LYP and M06-2X method, respectively, while Fig. S12 plots the experimental against the calculated (B3LYP) fluorescence emission maxima. From Figs. S10-12 data, it can be concluded that the UV-Vis absorption maxima calculated at various levels of DFT have almost the same error margins. In general, the UV-Vis absorption calculated at the M06-2X level shows a better correlation between the calculated and experimental data (Table 7 and Fig. S13). Otherwise, linear regressions of the calculated versus experimental UV-Vis results show that the almost same correlation coefficient (R^2) is obtained when the geometry of conformer **I** or **II** is used in UV-Vis calculations (Tables 6 and 7). A linear fit of absorption band positions in the calculated conformer **II** versus experimental spectra (Figures S10 and S11) gave correlation coefficients of 0.9773 and 0.8462 for the M06-2X and B3LYP method, respectively. Also, fluorescence emission maxima calculated at the DFT/B3LYP level using the geometry of conformer **I** and **II** (with and without intramolecular H-bond), show small deviations from those observed experimentally, with a correlation coefficient of 0.9536 and 0.9483, respectively. Experimental UV-Vis spectral data show that the maximum absorption of the investigated dyes occurs at 413–451 nm in ethanol as solvent. The theoretical results showed that TD-DFT/M06-2X method predict values at 366-391 nm. These results give the largest correlation coefficient (R^2) but at the same time yield the largest deviations of the absorption maxima of dyes as compared to the experimental ones. As these deviations represent a systematic underestimation of wavelengths, they can be easily cancelled using the appropriate scaling factor. In Figure

S13, an example of a scaled calculated UV-Vis spectrum of dye **4** in relation to the experimental spectrum in ethanol is given.

The influence of the substituent on the absorption maxima in the calculated UV-Vis spectra follows the trend in the experimental spectra. The bathochromic shifts are obtained by enhancing the electron donor properties of the diazo component. In this series of dyes, the introduction of electron donating substituent in the para position of the phenyl ring results in a significant bathochromic shift of the absorption and emission maximum according to unsubstituted dye in ethanol as solvent (Tables 6-8). Also, with the introduction of electron withdrawing substituent at the para position into phenyl ring, absorption and emission maxima shift hypsochromically according to unsubstituted dye.

In the optimized geometry of the conformer **I,** the plane of the amide group deviates from the plane of the molecule by ~25°. This deviation reduces delocalization of the electron density between these two parts of the molecule as can be seen from the FMO orbitals of dye **4**, Figure S14. The additional increase in the torsion angle of the amide group reduces the possibility of overlapping its π-orbital with the π-system of the phenylazo-pyridone moiety, as a result in the conformer **II**, which completely cancel delocalization between them. Therefore, it can be said that the effect of the amide group on the absorption maxima of the studied dyes is primarily inductive while the resonant effect is very small, in the conformer **I**, or completely absent, in the conformer **II**.

As can be seen from Tables 6-8 overall effect to absorption and emission maxima of the amide group is small, and the difference between conformer **I** and **II** is less than 7 nm. Therefore, from these correlations, it cannot be determined which conformer is dominant in the mixture.

Table 6 The experimental and B3LYP calculated absorption maxima of the conformers **I** and **II** of hydrazone tautomer of arylazo pyridone dyes (**1-9**) in ethanol as solvent.

	Conformer I			**Conformer II**			**Exp.**
	E_{abs} (eV)	λ_{max} (nm)	*f*	E_{abs} (eV)	λ_{max} (nm)	*f*	λ_{max} (nm)
1	2.780	459.1	0.9863	2.818	452.9	0.9351	450.6
2	2.720	454.3	0.9963	2.760	447.7	0.9446	443.7
3	2.896	428.1	1.0367	2.932	422.9	0.9891	428.9
4	2.990	414.6	0.9852	3.024	410.0	0.9448	418.7
5	2.933	422.8	1.0526	2.971	417.3	1.0124	422.2
6	2.910	426.1	1.0748	2.950	420.2	1.0363	422.9
7	2.977	416.3	1.1756	3.000	413.2	1.1422	421.9
8	2.980	416.0	1.1710	3.011	411.7	1.1476	413.0
9	2.851	434.9	1.1989	2.854	434.4	1.1748	422.8
R^2		0.8945			0.8462		

Table 7 The experimental and M06-2X calculated absorption maxima of the conformers **I** and **II** of hydrazone tautomer of arylazo pyridone dyes (**1-9**) in ethanol as solvent.

	Conformer I			**Conformer II**			**Exp.**
	E_{abs} (eV)	λ_{max} (nm)	*f*	E_{abs} (eV)	λ_{max} (nm)	*f*	λ_{max} (nm)
1	3.171	398.2	1.0809	3.226	391.0	1.0336	450.6
2	3.140	394.1	1.1036	3.195	387.2	1.0558	443.7
3	3.256	380.8	1.1273	3.309	374.7	1.0836	428.9
4	3.327	372.6	1.0741	3.381	366.7	1.0342	418.7
5	3.301	375.6	1.1543	3.356	369.5	1.1149	422.2
6	3.294	376.4	1.1914	3.349	370.2	1.1528	422.9
7	3.323	373.0	1.2492	3.373	367.5	1.2229	421.9
8	3.339	371.3	1.2708	3.390	365.7	1.2445	413.0
9	3.299	375.8	1.3161	3.338	371.4	1.2996	422.8
R^2		0.9778			0.9773		

Table 8 The experimental and B3LYP calculated fluorescence emission maxima of the conformers **I** and **II** of hydrazone tautomer of arylazo pyridone dyes (**1-9**) in ethanol as solvent.

	Conformer I			**Conformer II**			**Exp.**
	E_{em} (eV)	λ_{max} **(nm)**	***f***	E_{em} (eV)	λ_{max} **(nm)**	***f***	λ_{max} **(nm)**
1	2.371	536.5	0.9114	2.387	532.9	0.8585	555.0
2	2.317	531.6	0.9255	2.333	527.8	0.8783	544.2
3	2.451	506.0	0.9406	2.469	502.2	0.8907	515.2
4	2.550	486.3	0.8993	2.569	482.6	0.8635	499.1
5	2.482	499.5	0.9694	2.504	495.2	0.9251	503.8
6	2.459	504.1	0.9948	2.483	499.3	0.9494	506.5
7	2.560	484.0	1.0645	2.588	478.6	1.0471	500.3
8	2.565	483.5	1.0807	2.593	478.2	1.0569	490.7
9	2.586	479.5	1.2303	2.595	477.8	1.2056	484.8
R^2		0.9536			0.9483		

4. Conclusions

The aim of this work is solvatochromic analysis of new fluorescent dyes. In this paper, the synthesis and characterization of nine 5-(4-substituted phenylazo)-3-amido-6-hydroxy-4-methyl-2-pyridones are presented. FT-IR, ^{1}H NMR and ^{13}C NMR analysis have confirmed that all synthesized dyes exist in the tinctorial strongest tautomeric form, hydrazone form.

The Lippert-Mataga plot and the Reichardt-Dimroth plot showed satisfactory linear dependence when only a small number of solvents were included in the correlation,

indicating that multiparameter equation should be used. The analysis of the Stokes shift using the Kamlet–Taft equation shows that coefficient representing the basicity and dipolarity/polarizability of the solvent has a greater influence on spectral properties of the investigated dyes than coefficient representing the acidity. The similar behavior was obtained in the regression analysis when the absorption frequencies were used.

The effects of substituents on the absorption spectra of the investigated dyes were interpreted by using Hammett equation. The corresponding linear dependency with positive slope confirms the presence of hydrazone form in solvents used for analysis.

The selected dyes have almost the same UV-Vis spectrum in methanol and in acidic media, which confirmed that dyes are in hydrazone form. When the solution of dye **1** was made alkaline, a significant bathochromic shift was recorded in absorption spectra due to the formation of azo anion form.

The results of the conformational analysis with CPCM(ethanol)/M06-2X/6-311++G(d,p) method show that the most stable geometries of investigated dyes belong to the hydrazone tautomeric form. The most stable tautomer with respect to the mutual orientation of the amide group can exist in two conformational forms: with (I) and without (II) intramolecular H-bond and the ratio of conformers in the mixture depends on the properties of the solvents. Calculated absorption and emission spectra were analyzed to gain insight into the electronic structure of investigated molecules. Excellent correlations between computational and experimental data have been established.

Acknowledgement

Authors would like to acknowledge the financial support of Ministry of Education, Science and Technological Development of the Republic of Serbia under the Projects 45020, 172015, 172035, 175033 and 172013.

References

1. L. Racané**,** Z. Mihalic, H. Ceric, J. Popovic, V. Tralic-Kulenovic, Synthesis, structure and tautomerism of two benzothiazolyl azo derivatives of 2-naphthol: A crystallographic, NMR and computational study, Dyes Pigm. 96 (2013) 672-678.
2. H. Zollinger, Color Chemistry: Syntheses, Properties and Application of Organic Dyes and Pigments, 2nd ed. VCH, Weinheim (1991).
3. A. Alimmari, B. Bozic, D. Mijin, A. Marinkovic, N. Valentic, G. Uscumlic, Synthesis, structure and solvatochromic properties of some novel 5-arylazo-6-hydroxy-4-(4-methoxyphenyl)-3-cyano-2-pyridone dyes: Hydrazone-azo tautomeric analysis, Arab. J. Chem. 8 (2015) 269–278.
4. A. Panitsiri, S. Tongkhan, W. Radchatawedchakoon, U. Sakee, Synthesis and anion recognition studies of novel bis(4-hydroxycoumarin) methane azo dyes, J. Mol. Struct. 1107 (2016) 14-18.
5. E. Weglarz-Tomczak, Ł. Gorecki, Azo dyes–biological activity and synthetic strategy, Chemik 12 (2012) 1298-1307.
6. S.B. Novir, S.M. Hashemianzadeh, Quantum chemical investigation of structural and electronic properties of trans- and cis-structures of some azo dyes for dye-sensitized solar cells, Comput. Theor. Chem. 1102 (2017) 87–97.

7. N. Jaggi, M. Giri, K. Yadav, Absorption and fluorescence spectra of disperse red 19-An azo dye, Indian J. Pure Appl. Phy. 51 (2013) 833-836.
8. M.S. Aziz, H.M. El-Mallah, Electrical and optical properties of azo dyes, Indian J. Pure Appl. Phy. 47 (2009) 530-534.
9. A. Mohammadi, H. Ghafoori, B. Ghalami-Choobar, R. Rohinejad, Synthesis, solvatochromic properties and biological evaluation of some novel azo-hydrazone tautomeric dyes, J. Mol. Liq. 198 (2014) 44–50.
10. S. Shahab, F.H. Hajikolaee, L. Filippovich, M. Darroudic, V.A. Loiko, R. Kumar, M.Y. Borzehandani, Molecular structure and UV/Vis spectral analysis of new synthesized azo dyes for application in polarizing films, Dyes Pigm. 129 (2016) 9-17.
11. S. Abeta, Compatibility of acid dyes on nylon, Dyes Pigm. 18 (1992) 57-68.
12. R.J. Chudgar, J. Oakes, Dyes, Azo, In Kirk-Othmer Encyclopedia of Chemical Technology (2014) https://doi.org/10.1002/0471238961.01261503082104.a01.pub3.
13. N. Seto, Y. Kato, T. Fujimori, Colored curable compositions containing phthalocyanine and pyridone azo dyes and manufacture of color filters using them with excellent light and heat resistance, JP 2006071822, (2006), C.A. 144/2006 302015.
14. D.Ž. Mijin, G.S. Uščumlić, N.V. Valentić, A.D. Marinković, Synthesis of azo pyridone dyes, Hem. Ind. 65 (2011) 517-532.
15. M.S. Zakerhamidi, A. Ghanadzadeh, H. Tajalli, M. Moghadam, M. Jassas, R. Hosseini nia, Substituent and solvent effects on the photo-physical properties of some coumarin dyes, Spectrochim. Acta Part A **77** (2010) 337–341.
16. K. Hunger, Industrial Dyes, Chemistry, Properties, Applications Wiley-VCH, Weinheim, Cambridge, 648 (2003), ISBN:978-3-527-30426-4.

17. S. Tang, C. Zhao, G. Chen, G. Sun, A study on computerized selection of fluorescent dyes for environmentally friendly textile applications, Dyes Pigm. 165 (2019) 253-263.
18. P.P. Kasture, Y.A. Sonawane, R.N. Rajule, G.S. Shankarling, Synthesis and characterisation of benzothiazole-based solid-state fluorescent azo dyes, Color. Technol. 126 (2010) 348–352.
19. S. Abou-Hatab, V.A. Spata, S.Matsika, Substituent Effects on the Absorption and Fluorescence Properties of Anthracene, J. Phys. Chem. A 121 (6) (2017) 1213-1222.
20. J. Yoshino, A. Furuta, T. Kambe, H. Itoi, N. Kano, T. Kawashima, Y. Ito, M. Asashima, Intensely Fluorescent Azobenzenes: Synthesis, Crystal Structures, Effects of Substituents, and Application to Fluorescent Vital Stain, Chem. Eur. J. 16 (2010) 5026 – 5035.
21. J. Yoshino, N. Kano, T. Kawashima, Fluorescent azobenzenes and aromatic aldimines featuring an N–B interaction, Dalton Trans. 42 (2013) 15826.
22. M.A. Satam, R.K. Raut, N. Sekar, Fluorescent azo disperse dyes from 3-(1,3-benzothiazol-2-yl)naphthalen-2-ol and comparison with 2-naphthol analogs, Dyes Pigm. 96 (2013) 92-103.
23. T. Aysha, M. El-Sedik, S.A. El Megied, H. Ibrahim, Y. Youssef, R. Hrdina, Synthesis, spectral study and application of solid state fluorescent reactive disperse dyes and their antibacterial activity, Arab. J. Chem. 12 (2016) 225-235.
24. S. Shinde, N. Sekar, Synthesis, spectroscopic characteristics, dyeing performance and TD-DFT study of quinolone based red emitting acid azo dyes, Dyes Pigm. 168 (2019) 12-27.

25. J.M. Mirković, B.Đ. Božić, D.R. Mutavdžić, G.S. Ušćumlić, D.Ž. Mijin, Solvent and structural effects on the spectral shifts of 5-(substitutedphenylazo)-3-cyano-6-hydroxy-1-(2-hydroxyethyl)-4-methyl-2-pyridones, Chem. Phys. Lett. 615 (2014) 62–68.
26. S.T. Abdel-Halim, Effect of solvent on absorption and fluorescence spectra of a typical fluorinated azo dye for its acidic and basic structures, Spectrochim. Acta Part A 82 (2011) 253– 259.
27. D. Debnath, S. Roy, Bing-Han Li, Chia-Her Lin, T. K. Misra, Synthesis, structure and study of azo-hydrazone tautomeric equilibrium of 1,3-dimethyl-5-(arylazo)-6-amino-uracil derivatives, Spectrochim. Acta A. 140 (2015) 185–197.
28. D. Magde, G.E. Rojas, P.G. Seybold, Solvent Dependence of the Fluorescence Lifetimes of Xanthene Dyes, Photochem. Photobiol. 70 (1999) 737-744.
29. S.J. Porobić, A.D. Krstić, D.J. Jovanović, J.M. Lađarević, Đ.B. Katnić, D.Ž. Mijin, M. Marinović-Cincović, Synthesis and thermal properties of arylazo pyridone dyes, Dyes Pigm. 170 (2019) https://doi.org/10.1016/j.dyepig.2019.107602.
30. J.M. Dostanic, D.R. Loncarevic, P.T. Bankovic, O.G. Cvetkovic, D.M. Jovanovic, D. Ž. Mijin, Influence of process parameters on the photodegradation of synthesized azo pyridone dye in TiO_2 water suspension under simulated sunlight, J. Environ. Sci. Health A Tox. Hazard. Subst. Environ. Eng. 46 (2011), 70-79.
31. M.J. Frisch, G.W. Trucks, H.B. Schlegel, G.E. Scuseria, M.A. Robb, J.R. Cheeseman, G. Scalmani, V. Barone, B. Mennucci, G.A. Petersson, H. Nakatsuji, M. Caricato, X. Li, H.P. Hratchian, A.F. Izmaylov, J. Bloino, G. Zheng, J.L. Sonnenberg, M. Hada, M. Ehara, K. Toyota, R. Fukuda, J. Hasegawa, M. Ishida, T. Nakajima, Y. Honda, O. Kitao, H. Nakai, T. Vreven, J.A. Montgomery, Jr., J.E. Peralta, F. Ogliaro, M.

Bearpark, J.J. Heyd, E. Brothers, K.N. Kudin, V.N. Staroverov, R. Kobayashi, J. Normand, K. Raghavachari, A. Rendell, J.C. Burant, S.S. Iyengar, J. Tomasi, M. Cossi, N. Rega, J. M. Millam, M. Klene, J.E. Knox, J.B. Cross, V. Bakken, C. Adamo, J. Jaramillo, R. Gomperts, R.E. Stratmann, O. Yazyev, A.J. Austin, R. Cammi, C. Pomelli, J.W. Ochterski, R.L. Martin, K. Morokuma, V.G. Zakrzewski, G.A. Voth, P. Salvador, J.J. Dannenberg, S. Dapprich, A.D. Daniels, Ö. Farkas, J.B. Foresman, J.V. Ortiz, J. Cioslowski, and D.J. Fox, Gaussian 09, Revision D.01. Wallingford CT: Gaussian, Inc.; 2009.

32. M. P. Andersson, P. Uvdal, New Scale Factors for Harmonic Vibrational Frequencies Using the B3LYP Density Functional Method with the Triple-ζ Basis Set 6-311+G(d,p), J. Phys. Chem. A 109 (12) (2005) 2937–2941.
33. R. Dennington, T.Keith, J. Millam, GaussView, Version 5.0.9. Shawnee Mission, KS: Semichem Inc.; 2009.
34. A. Saeed, G. Shabir, New fluorescent symmetrically substituted perylene-3,4,9,10-dianhydride-azohybrid dyes: Synthesis and spectroscopic studies, Spectrochim. Acta Part A 133 (2014) 7–12.
35. X. Ma, R. Sun, J. Cheng, J. Liu, F. Gou, H. Xiang, X. Zhou, Fluorescence Aggregation-Caused Quenching versus Aggregation-Induced Emission: A Visual Teaching Technology for Undergraduate Chemistry Students, J. Chem. Educ. 93 (2016) 345-350.
36. J. Jayabharathi, V. Thanikachalam, M.V. Perumal, K. Jayamoorthy, Solvatochromic Studies of Fluorescent Azo Dyes: Kamlet-Taft (π*, α and β) and Catalan (Spp, SA and SB) Solvent Scales Approach, J. Fluoresc. 22 (2012) 213–221.

37. M. Ravi, A. Samanta, and T.P. Radhakrishnan, Excited State Dipole Moments from an Efficient Analysis of Solvatochromic Stokes Shift Data, J. Phys. Chem. 98 (1994) 9133-9136.

38. M.J. Kamlet, J.M. Abboud, R.W. Taft, An Examination of Linear Solvation Energy Relationships, Prog. Phys. Org. Chem. 13 (1981) 485-630.

39. J.M. Abboud, M.J. Kamlet, R.W. Taft, The solvatochromic comparison method. 6. The π* scale of solvent polarities, J. Am. Chem. Soc. 99 (1977) 6027-6038.

40. M.J. Kamlet, R.W. Taft, The solvatochromic comparison method. I. The β-scale of solvent hydrogen-bond acceptor (HBA) basicities, J. Am. Chem. Soc. 98 (1976) 377-383.

41. M.J. Kamlet, R.W. Taft, Linear solvation energy relationships. Part 3. Some reinterpretations of solvent effects based on correlations with solvent π* and α values J. Chem. Soc., Perkin Trans. 2 (1979) 349-356.

42. Y. Smortsova, H. Oher, F.A. Miannay, R. Vanel, J. Dubois, O. Kalugin, A. Idrissi, Solvatochromic effects on a class of indoline derivatives organic photosensitizers: About the influence of hydrogen-bond acceptor and donor abilities parameters, J. Mol. Liq. 245 (2017) 76–84.

43. F. Gillanders, L. Giordano, S.A. Díaz, T.M. Jovin, E.A. Jares-Erijman, Photoswitchable fluorescent diheteroarylethenes: Substituent effects on photochromic and solvatochromic properties, Photochem. Photobiol. Sci., 2014, 13, 603

44. J. Lađarević, B. Božić, L. Matović, B. Božić, Nedeljković, D. Mijin, Role of the bifurcated intramolecular hydrogen bond on the physico-chemical profile of the novel azo pyridone dyes, Dyes Pigm. 162 (2019) 562-572.

45. A.G. Gilani, V. Taghvaei, E.M. Rufchahi, M. Mirzaei, Tautomerism, solvatochromism, preferential solvation, and density functional study of some heteroarylazo dyes, J. Mol. Liq. 273 (2019) 392-407.
46. R. Karpicz, V. Gulbinas, A. Undzenas, Picosecond Spectroscopic Studies of Tautomers of a Bisazo Compoundin Solutions, J. Chin. Chem. Soc. 47 (2000) 589-595.
47. J. Mirković, J. Rogan, D. Poleti, V. Vitnik, Ž. Vitnik, G. Uščumlić, D. Mijin, On the structures of 5-(4-, 3- and 2-methoxyphenylazo)-3-cyano-1-ethyl-6-hydroxy-4-methyl-2-pyridone: An experimental and theoretical study, Dyes Pigm. 104 (2014) 160-168.
48. V.D. Vitnik, Ž.J. Vitnik , B.Đ. Božić, N.V. Valentić, S.P. Dilber, D.Ž. Mijin, G.S. Uščumlić, Experimental and theoretical insight into the electronic properties of 4-aryl-5-arylazo-3-cyano-6-hydroxy-2-pyridone dyes, Color. Technol. 133 (2017) 223-233.
49. D. Mijin, B. Božić. J. Lađarević, L. Matović, G. Uščumlić, V. Vitnik, Ž. Vitnik, Solvatochromism and quantum mechanical investigation of disazo pyridone dye, Color. Technol. 134 (2018) 478–490.
50. J. Dostanić, D Mijin, G. Uščumlić, D.M. Jovanović, M. Zlatar and D. Lončarević, Spectroscopic and quantum chemical investigations of substituent effects on the azo-hydrazone tautomerism and acid-base properties of arylazo pyridone dyes, Spectrochim. Acta A 123 (2014) 37-45.
51. N. Ertan and F. Eyduran, The synthesis of some hetarylazopyridone dyes and solvent effects on their absorption spectra, Dyes Pigm. 27 (1995) 313-320.

52. G. A. Jeffrey, An Introduction to Hydrogen Bonding, Oxford University Press, New York, 1997.

53. V.M. Arsovski, B.Dj. Božić, J.M. Mirković, V.D. Vitnik, Ž.J. Vitnik, W.M.F. Fabian, S.D. Petrović, D.Ž. Mijin, Spectroscopic and quantum mechanical investigation of N,N'-bisarylmalonamides: solvent and structural effects, J. Mol. Model. 20 (2014) 1-16.

54. P.I. Nagy, Competing Intramolecular vs. Intermolecular Hydrogen Bonds in Solution, Int. J. Mol. Sci. 15 (2014) 19562-19633.

55. C.J. Cramer, D.G. Truhlar, Implicit Solvation Models: Equilibria, Structure, Spectra, and Dynamics, Chem. Rev. 99 (1999) 2161-2200.

56. C.P. Kelly, C.J. Cramer, D.G. Truhlar, Adding Explicit Solvent Molecules to Continuum Solvent Calculations for the Calculation of Aqueous Acid Dissociation Constants, J. Phys. Chem. A 110 (2006) 2493–2499

57. E.F. da Silva, H.F. Svendsen, K.M. Merz, Explicitly Representing the Solvation Shell in Continuum Solvent Calculations, J. Phys. Chem. A 113 (2009) 6404–6409.

58. R. J. Abraham, L. Griffiths, M. Perez, ^{1}H NMR spectra part 31: ^{1}H chemical shifts of amides in DMSO solvent, Magn. Reson. Chem. 52 (2014) 395–408.

Highlights

The absorption and emission spectra of nine arylazo pyridone dyes were recorded.

The solvent effects on the absorbance and emission spectral shift were analyzed.

The conformational analysis showed that the investigated dyes are in hydrazone form.

The existence of two conformational forms of hydrazone tautomer was confirmed.

Excellent correlations between computational and experimental data were established.

Declaration of interests

☒ The authors declare that they have no known competing financial interests or personal relationships that could have appeared to influence the work reported in this paper.

☐The authors declare the following financial interests/personal relationships which may be considered as potential competing interests: